

Ultradilute Ag-aquasols with extraordinary bactericidal properties: role of the system Ag–O–H₂O

R. Roy¹, M. R. Hoover*¹, A. S. Bhalla¹, T. Slaweki¹, S. Dey², W. Cao², J. Li² and S. Bhaskar²

We first establish the literature on the use of ultradilute aquasols as extraordinary, powerful, bactericidal inorganic agents equal to most commercial antibiotics. These findings provide the rationale for a major role for inorganic materials scientists to contribute the insights unique to their field for new, safer health vectors. The focus of this preliminary paper is exclusively on the materials science of 2-phase stable sols at ultradilute concentrations near 1 at.-ppm. We analyze the solid and liquid phases for the first time in detail using standard materials science analysis tools. The solid phase is analyzed using DTA, TGA, XRD, SEM, and TEM, and the liquid water phase is analyzed using FTIR, UV–VIS, and Raman spectroscopy. There are at least three crystalline phases in the system Ag–O: Ag, Ag₂O, and Ag₄O₄, which are stable in air. In an aqueous environment between 0 and 100°C there is evidence that various combinations of metal, oxides, and possible ‘oxy-hydroxide’ complexes exist. Similarly, data from Raman and UV–VIS spectroscopy show definite changes in the structure of the water host. These results, in a preliminary way, are parallel to the many empirical observations made by physicians for the last 100 years on the use of metallic silver and water in various combinations for human health.

Keywords: Silver, Silver aquasols, Solid particle size and composition, Structure of liquid phase, Raman spectroscopy, UV–VIS, FTIR

Introduction

Summary of known biological activities of silver in contact with water

For thousands of years in various countries, especially India, silver has been used for what was empirically known to be its bactericidal properties – to keep water, and often foods, safer. A recent paper by Das *et al.* provides the remarkable datum that some 275 000 kg of edible metallic silver foil are consumed every year (in food) in India.¹ No known adverse health effects have ever been recorded. This epidemiological evidence that silver as a metal is not toxic in any way needs no further comment. Further support for the obvious safety of consuming metallic silver (Ag⁰) is in the worldwide consumption of (so-called) silver colloids, often made at home in primitive electrochemical cells by probably some millions of citizens, again with no ill effects. Regrettably the distinction between Ag⁰ and Ag⁺¹ as an ion has not been made in many medical studies, and the important distinction between soluble silver as an ion or organic complex is not appreciated.

Starting in Greece and the Roman Empire in Europe, the use of silver by the wealthier classes for similar purposes, and for making utensils for feeding children (and adults) are certainly due to the same experience. In the USA during the Westward expansion, cowboys, mining camps, and various outposts regularly dropped silver coins into the drinking water barrel to keep it safe. By 1900 a variety of devices, medications, etc., were widely advertised for various health remedies. Figure 1 shows some advertisements for silver ‘medications.’ No scientific papers challenging the clinical efficacy of these earlier practices appeared. But over the next several decades following the discovery of penicillin, the emergence of the organic, biochemical ‘antibiotics’ caused the disappearance of these older (albeit much cheaper) remedies, yet silver stents and other state of the art devices have been in continuous use in major hospitals for some decades, attesting to the bactericidal efficacy of the metal. As recently as the American Physical Society meeting in Baltimore, March 2006, Storey provided data on another recent example of the use of coatings of metallic silver on various prosthetic implants.²

It is less known that metallic silver has a second major use in human health – for the reduction of pain. In this application, the property involved is the high electrical conductivity and chemical inertness of the metal. Pain is

¹The Pennsylvania State University, 102 Materials Research Laboratory, University Park, PA 16802

²Department of Materials Science, Arizona State University, Tempe, AZ 85287

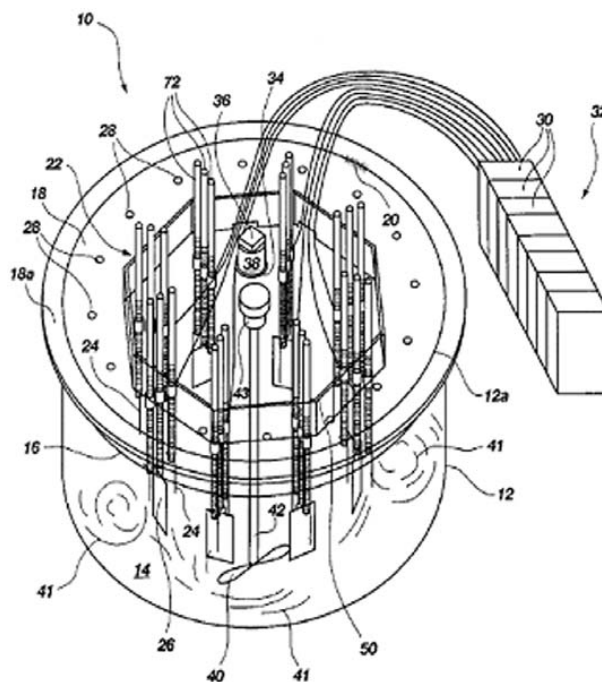
*Corresponding author, email mrh19@psu.edu

As noted, metallic aquasols can be prepared by various routes: by chemical reduction from ionic solutions, by electrolysis, or by striking a high-amperage arc between metal electrodes under the liquid. Home kits are available at health food stores to prepare such metallic aquasols using 9 V electrolysis. In 2002, a new process was patented for preparing such silver sols by electrolysis utilizing a unique AC voltage drop of ~10 kV between silver electrodes suspended in a glass chamber (Fig. 2). Holladay et al. show the electrode arrangement.⁹ The biological properties of these sols at concentrations of 10–30 wt-ppm of silver in pure water have been shown to be most remarkable in a series of studies at several different institutions worldwide. These biological properties were the major reason for choosing this particular set of sols as one example of this class of materials.

Table 1 shows a comparison of the MIC (minimum inhibitory concentrations) of ~1 at.-ppm silver sol in pure water with the most prominent antibiotics used worldwide as fully established in both *in vitro* and *in vivo* trials.¹⁰ Not only is this radically different antibiotic material more or less equal to the traditional biochemical antibiotics, it has the unique advantage that bacteria do not mutate to destroy its activity. Moreover, when used alongside a traditional antibiotic, as shown in Table 2, the silver aquasol has a synergistic effect thereby extending the life of the efficacy of several antibiotics tenfold.¹¹ Much of our work has used these materials as examples of silver aquasols. Such biological data provide the paradigm-challenging justification for studying this extraordinary family of materials as potential leaders of a new class of health vectors.

Previous work on materials science of silver sols

There is an enormous confusion in the literature on what condensed phases exist in the system Ag–O–H₂O. The ICDD X-ray data file refers to some five or six oxides of silver (Ag₂O₃, AgO, 2AgO, Ag₂O, Ag₃O₄) of different stoichiometries. The Landolt Bornstein metal–oxygen phase diagram compilation shows Ag, Ag₂O, AgO. The solubility of oxygen in the silver lattice is noticeable and oxygen substantially lowers the melting point from 945 to 929°C. A phase labeled Ag₄O₄, a brownish powder, is available commercially because of its use in the manufacturing of batteries, but it is relatively unknown in the



2 Colloidal silver apparatus (US Patent 6,214,229) 10 apparatus, 12 container, 12a lip, 14 fluid, 16 upper surface, 18 lid, 18a perimetric overhang, 20 hinge, 22 sets of electrodes, 24 upper electrodes, 26 lower electrodes, 28 air inlet openings, 30 transformer, 32 transformer bank, 34 air outlet openings, 36 fan, 38 air outlet channel, 40 impeller, 41 internal current, 42 impeller rod, 43 impeller motor, 50 non-conductive housing, 56 conductive electrode holder, 58 female-threaded mounts, 62 conductive connector, 66 electrical leads, 68 parallel connector

scientific literature. Virtually nothing is known of the binary system Ag–H₂O: no hydroxides have ever been reported, nor have any allusions been made to any oxyhydroxides since Ag is nominally monovalent.

Obviously all these questions and many more need to be answered more definitively to begin to explain in detail the mechanism for the remarkable healing properties of such silver sols. This is the mandate for a thorough phase equilibrium study of the system Ag–O–H₂O, for which the present work is a first step.

Table 1 Minimum inhibitory concentrations (MIC) of ASAP silver sol in water¹⁰

Organism	Antimicrobial					
	Tetracycline	Oxfloxacin	Penicillin G	Cefaperazone	Erythromycin	ASAP
S. pyogenes	0.625/>5	1.25/2.5	>5.0	0.313/1.25	0.003/0.019	2.5/5.0
S. mutans	0.625/>5	2.5/>5.0	0.521/>5	1.25/>5	0.009/0.019	2.5/10.0
S. gordonii	0.156/0.625	2.5/5.0	0.009/0.039	1.25/1.25	0.005/0.019	2.5/10.0
S. pneumoniae	0.078/0.625	2.5/2.5	0.019/0.019	0.313/0.313	0.002/0.004	2.5/2.5
S. faecalis	0.313/>5	1.25/5.0	5.0/>5.0	>5.0	0.009/1.25	10.0/10.0
S. aureus	0.313/>5	0.417/0.625	2.5/>5.0	5.0/5.0	0.039/>5.0	5.0/5.0
P. aeruginosa	0.78/5	0.156/0.313	0.13/>5.0	2.5/5.0	2.5/5.0	1.67/5
E. coli	1.67/>5	0.104/0.156	>5.0	0.625/>5.0	5.0/>5.0	2.5/2.5
E. aerogenes	>5	0.078/0.156	>5.0	2.92/>5.0	>5.0	2.5/2.5
E. cloacae	1.67/>5	0.156/0.156	>5.0	>5.0	>5.0	2.5/5.0
S. tiphimurium	1.25/>5	0.078/0.156	>5.0	1.25/2.5	5.0/>5.0	2.5/5.0
S. arizona	0.625/>5	0.078/0.078	>5.0	0.833/>5.0	4.17/>5.0	2.5/5.0
S. boydii	1.25/>5	0.078/0.156	>5.0	0.625/0.625	5.0/>5.0	1.25/1.25
K. pneumoniae	2.5/>5	0.417/0.625	>5.0	>5.0	>5.0	2.5/2.5
K. oxytoca	1.25/>5	0.104/0.156	>5.0	1.25/>5.0	>5.0	1.25/1.25

Goal of this work

This study was limited to characterization of the two phases of the sol, i.e. solid and liquid. The overall goal was to determine the composition and the structure of each phase in a specific and/or typical silver aquasol.

Experimental

Samples examined

We examined some half a dozen commercially available ‘silver colloid’ products from various manufacturers, but we spent considerably more time and attention on the product of a new manufacturer (American Biotech Laboratories). This product was made by the extraordinary process of using very high voltage (~10 kV) fields for electrolysis as noted above. (See Fig. 2, US Patent 6,214,299, and its legend.⁹)

Understanding the experimental limitations

In this study we dealt with only ultradilute sols in the range of about 1 at.-ppm of silver. Up to now the influence on the liquid phase water structure has been assumed to be *de minimis*. Likewise the solid phase was considered to be too low in concentration to allow detailed compositional and structural characterization in the sol state. Transferring to the conditions required for the necessary analysis largely by electron microscopy opened up some real insuperable limitations. Simple minded acceptance of the data could well be wholly misleading because the vacuum and the electron beam change what is actually present in the claimed liquid–solid dispersion – the colloid, or sol. We address this problem below. We chose reliable commercial products which had demonstrated outstanding and powerful antibiotic effects in easily reproduced *in vitro* experiments. We attempted to definitively characterize the size, composition and structure of the solid phases, as well as the ‘structure’ of the aqueous dispersion, through the use of modern analytical techniques.

Results

Concentration and composition of total ‘impurities’ (solid and in solution)

The concentration of silver in the dispersion was determined using standard ICP analysis. The total

concentrations of silver in the starting water and in the sols claimed by the manufacturers, 0, 10, 22, and 32 wt-ppm, were confirmed within 1 ppm. The water phase was found to be very pure with the concentration of very few other elements above 10 ppb.

Characterization of solid phase: possible candidate/phases

The Noble metals, Ag, Au, Pt, etc., are nearly universally assumed to not form any oxides at all. There has been an explosion of recent papers on preparing ‘nanoparticles’ of Ag, Au, Pt, etc. (usually as aqueous sols), and even indeed modifying their shape by exposing them to different wavelength radiation.¹² These papers generally made the assumption that these nanoparticulate materials do not oxidize on contact with air and water. This may be true. Yet Roy showed in a series of papers in 1967–71 that both Au and Pt can form binary oxides, and various ternary oxides. He studied their stabilities and concluded that probably in the ambient atmosphere these metals owe their ‘noble’ or chemically resistant character to a thin coating of their own oxides. Müller and Roy and Müller *et al.* provided XRD data on Au, Pt, Rh, and Re oxides.^{13,14} Regrettably, they did not study Ag, but it would appear to be certain that metallic silver in the typical laboratory ambient is coated with some oxide layer.

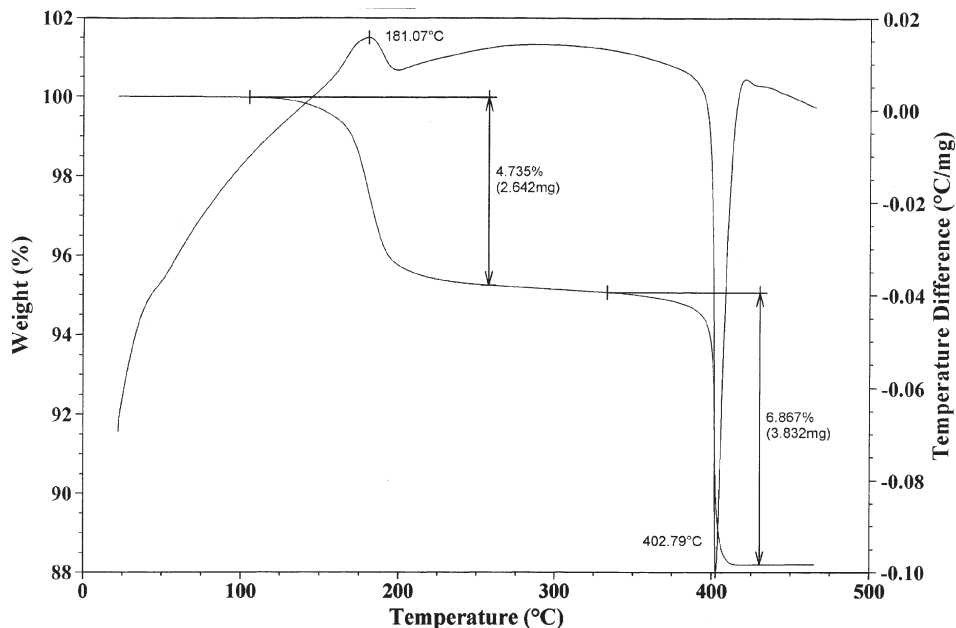
In the case of silver the common scientific literature recognizes mainly the existence of the one silver oxide, Ag₂O. But the world of the technology (especially battery technology) routinely deals in a silver oxide phase reported to be Ag₄O₄, with some speculation that it contains not divalent silver but a mixture of Ag¹⁺ and Ag³⁺. We have worked with commercial samples of Ag₄O₄. The decomposition of Ag₄O₄ to Ag₂O and then to Ag was studied by DTA and TGA. The results in Fig. 3 show the two-step decomposition. Once formed, the Ag₄O₄ is unlikely to be reduced in any normal laboratory or home ambient. However, no measurements have been made of its stability in water.

TEM studies carried out on the Ag₄O₄ powder showed how the powder, originally crystalline, reacts with the beam and is reduced in the same two-step manner in a few seconds; first to a more ‘dense’ phase

Table 2 Synergism of silver–water dispersion with antibiotics¹¹

Antibiotic discs (µg)	<i>E. coli</i> (MDR)	<i>Ps. aeruginosa</i> (MDR)	MRSA	<i>S. aureus</i> 6538 P	<i>S. typhi</i>	<i>Sh. flexneri</i>	<i>B. subtilis</i>
Amikacin	–	–	Syn.	Add.	–	–	Add.
Amoxicillin	–	–	Ant.	Add.	Add.	Add.	Add.
Carbenicillin	–	–	Add.	Add.	Add.	Add.	Add.
Cefperazone	–	–	Syn.	Add.	Add.	Add.	Add.
Ceftizidime	Syn.	Syn.	Add.	Add.	Add.	Add.	Add.
Ciprofloxacin	–	–	Add.	Add.	Add.	Add.	Add.
Clindamycin	–	–	Add.	Add.	–	Add.	Add.
Doxycycline	–	–	Add.	Add.	Add.	Add.	Add.
Erythromycin	–	–	Add.	Add.	–	Add.	Add.
Gentamycin	Add.	–	Add.	Add.	Add.	Add.	Add.
Kanamycin	Syn.	–	Add.	Add.	Add.	Add.	Add.
Nalidixic acid	–	–	–	Add.	Add.	Add.	Add.
Oxacillin	–	–	Ant.	Add.	–	Add.	Add.
Penicillin G	–	–	Add.	Add.	Add.	Add.	Add.
Rifampin	Add.	Add.	Add.	Add.	Add.	Add.	Add.
Streptomycin	Add.	–	Add.	Add.	Add.	Add.	Add.
Tetracycline	–	–	Add.	Add.	Add.	Add.	Add.
Tobramycin	Add.	–	Add.	Add.	Add.	Add.	Add.
Trimethoprim	–	–	Add.	Add.	Add.	Add.	–

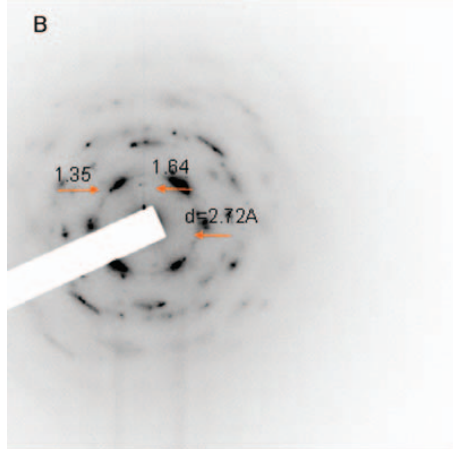
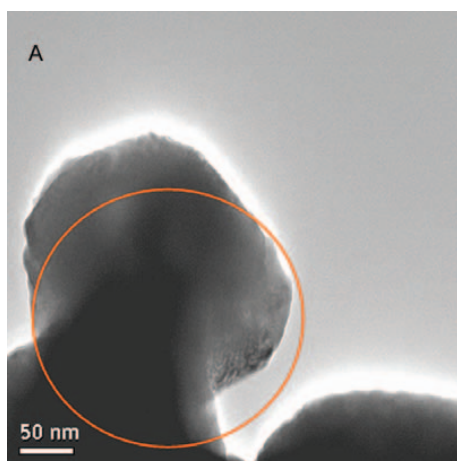
MDR=multi-drug resistant; Add.=additive; Syn.=synergistic; Ant.=antisynergistic.



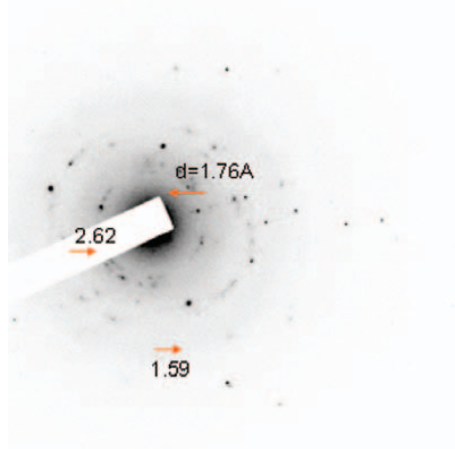
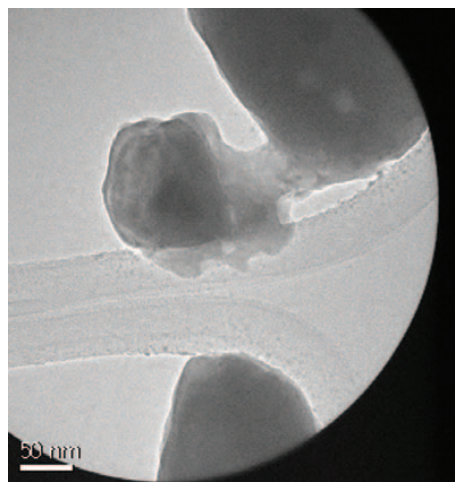
3 Decomposition of Ag₄O₄ to Ag₂O then Ag as shown by DTA and TGA studies

and finally to very dense small particles – possibly reflecting the same steps as above from Ag₄O₄ to Ag₂O to Ag (Figs. 4–7).

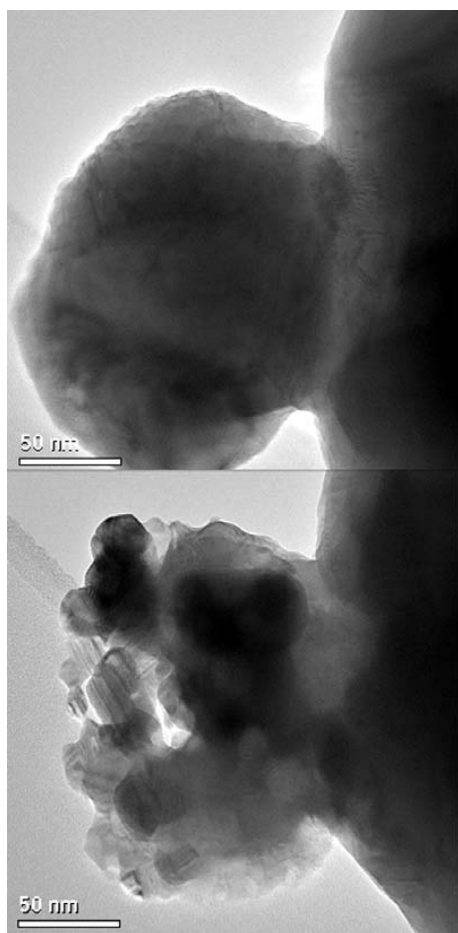
The second peak in both DTA and TGA compounds is caused by the decomposition of Ag₂O to silver and oxygen, at about 420°C in the DTA. (This is also near the



4 TEM image and small area nanodiffraction pattern confirming presence of Ag₄O₄; note diffraction spots are broad and elongated, which indicates a range of distribution of the crystal interplane distances

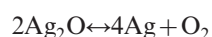


5 TEM image showing area selected (~0.5 μm region) and corresponding SAD pattern showing that particles are crystalline: spots from different crystal planes probably originate from different crystals



6 Particles are sensitive to electron beam radiation: TEM images before (top) and after intensified beam radiation for seconds clearly show changes in shape and diffraction contrast

minimum temperature which must be attained to remove the tarnish from silver without any chemical treatment.) Of course it is not the equilibrium temperature of 195°C (468 K) for dissociation which can be deduced from the values cited in the chemical literature for the reaction



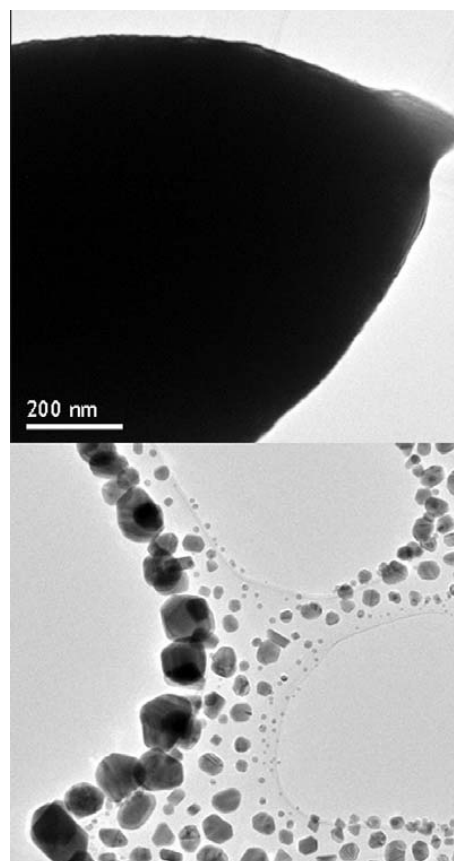
where equilibrium temperature $T = \Delta H_{\text{rxn}} / \Delta S_{\text{rxn}} = 62.2 \text{ kJ} / 0.133 \text{ kJ K}^{-1} = 468 \text{ K} = 195^\circ\text{C}$, assuming that ΔH is $14.9 \text{ kcal mol}^{-1}$.

However, this equilibrium does not apply to any sol. It is the activity of oxygen in the water, with and without electric fields, which is determinative of which phase is thermodynamically stable in the presence of water, not that which forms in the sol-making process or in treatments at the low temperature (0 to $<100^\circ\text{C}$) which are involved in the preparation and use of such sols in health applications.

Moreover these solid phases refer only to those which have some range of thermodynamic stability. Many, often intermediate, metastable phases may well form. However, so far no characterization data have been presented on any such phases, which may very well exist, and we have not encountered any such with any degree of reproducibility.

Size and crystal structure of solid phase from sol

For the analysis of the size and crystal structure of the particles in the sols we were forced to electron

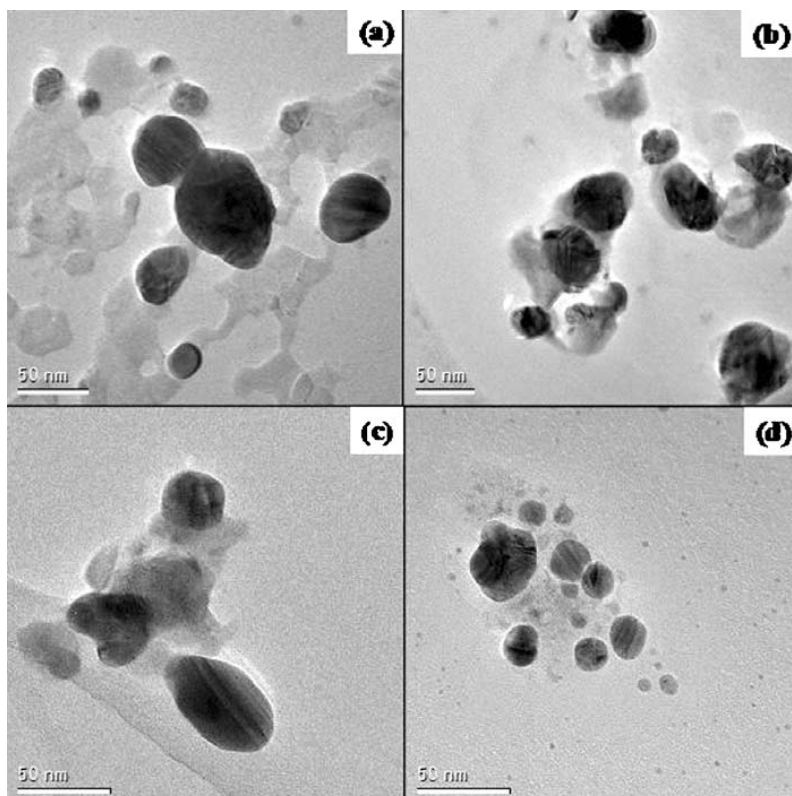


7 Irradiation with intensified electron beam can generate an array of nanoparticles, as shown by the ‘blob’ and multiple small crystals formed from the original particle aggregation: these particles are have probably been reduced to Ag

microscopy methods. We realized fully the limitations of this technique since one has to separate the solid phase present in 1 ppm concentrations, subject it to a 10^{-9} torr vacuum as well as to the heat from the electron beam. The following threats exist. First, particles may aggregate upon drying so that the apparent ‘particle size’ must be carefully interpreted. Second, the necessary vacuum in the SEM and TEM can alter the phase present, especially if it is a hydroxide, an oxide or a carbonate. Third, the temperature of the beam can, likewise, cause phase changes in such material. Of course, much of the data will be unaffected by these constraints, and the possibilities for some others will be *de minimis*.

Keeping these caveats in view, data obtained in SEM, environmental TEM, TEM, SAED and EELS (facilities chiefly at ASU, with some work with cryo-TEM at the University of Washington) are summarized below. Several scores of such images have been recorded, and a selection has had to be made for each point.

For TEM analysis, several drops of liquid water were placed on a common TEM copper grid covered with a carbon lacey film. The copper grid was dried in a desiccator in air to evaporate the water then inserted into the microscope at 10^{-9} torr vacuum. The comparison among several different available silver sols is shown in Fig. 8. These images show a series of TEM images of a variety of particles obtained from these sols. The ‘particles’ or clusters are all in the size range of



8 TEM bright field images from different silver sols containing *a* ASAP 10 ppm, *b* GNC, *c* Silverado, *d* Bioorganic

10–50 nm with a median near 30 nm. Further HRTEM examination reveals that a large number of silver particles appear to be single crystal, although distorted and twinned crystal lattices were also observed (Fig. 9).

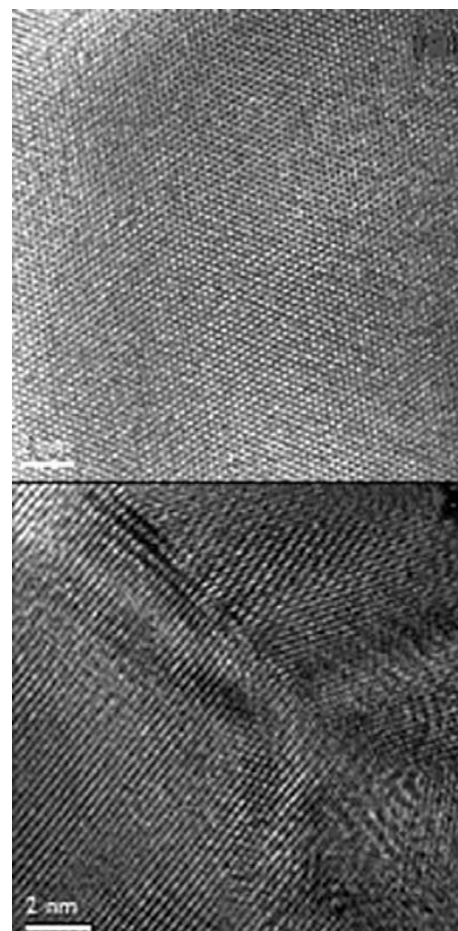
Electron diffraction studies were carried out on the aforementioned silver sol samples to identify possible silver phases. Figures 10 and 11 are two of dozens of such images which show one typical SAED pattern for metallic silver particles and a different pattern for samples in which some oxides appear. The results indicated that, in addition to the elemental silver phase, the dominant phase identified, often possible silver oxide phases, some with strange stoichiometries (based on the ICDD data), were identified. Much further investigation is required to confirm these results, but a second, oxidic, phase appears in many contexts.

We considered alternative methods of separating out sufficient solid phase from the sol by centrifugation at the maximum force available. Special sols were made with 200 ppm silver by the same process. These were evaporated and dried below 100°C under blankets of N₂ at reduced pressure and the thin layers of powder (when formed) were X-rayed. Only from the 200 ppm sol were we able to get enough samples. But in spite of extraordinary precautions, a large fraction of the final dried phase turned out to be Ag₂CO₃, with Ag₂O.

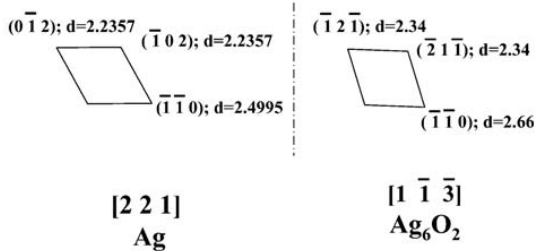
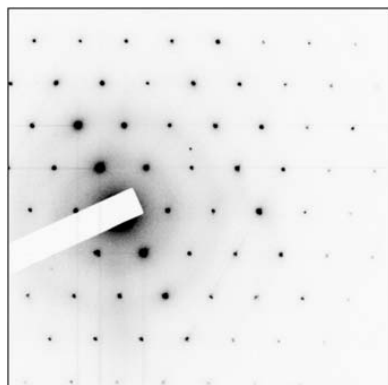
Due to the nature of the oxygen in the particles four hypotheses can be tested.

- (i) All particles are pure metallic silver
- (ii) All particles are pure silver oxide
- (iii) Particles have metallic silver cores with a “shell” of oxide
- (iv) Ag is partially internally oxidized, i.e. in metastable solid solution.

We have conducted a series of experiments using electron energy loss spectroscopy (EELS) across the



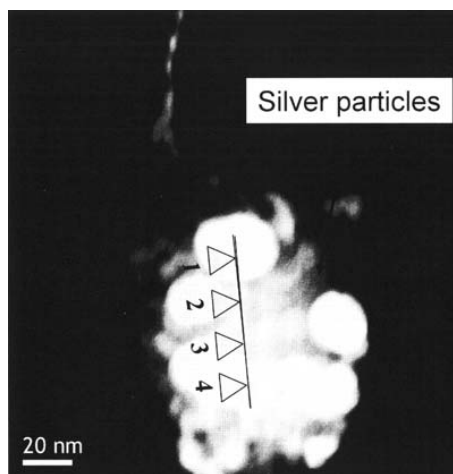
9 HRTEM images of ASAP plus 22 ppm silver phase, showing regions characterised by well crystallised single crystal (top) and distorted (bottom) lattices



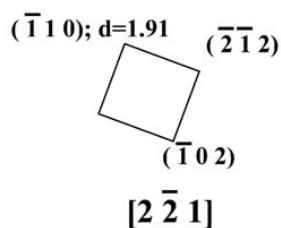
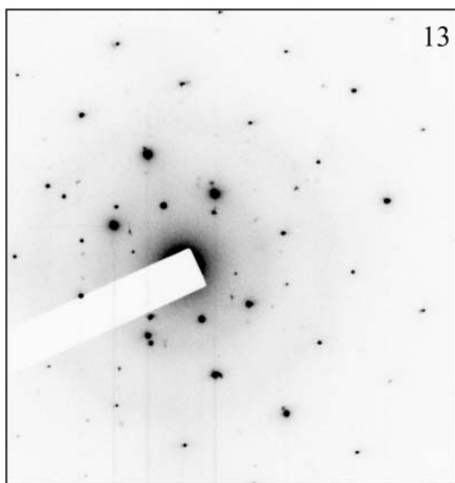
- Two possible phases (d spacing in Angstrom)
 - Hexagonal Ag; space group P6₃/mmc (194)
 - Hexagonal Ag₆O₂; space group P-31m (162)

10 Typical electron diffraction pattern for all five silver sol samples (1 or 2 random grains/sample): indexed patterns have two possible phase assignments

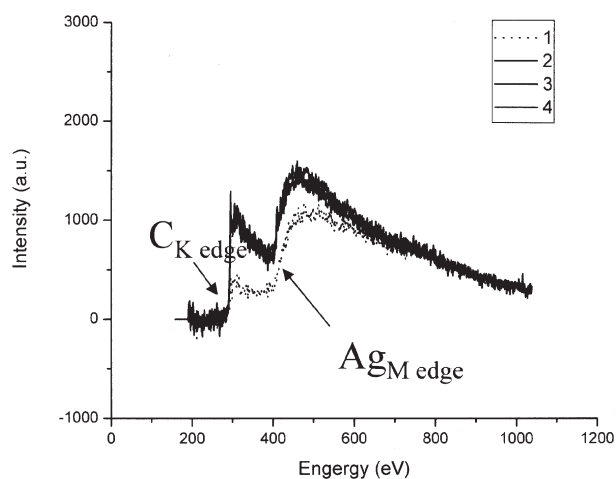
particles in an attempt to determine the nature of the oxygen. However, no oxygen was actually detected for the samples on which EELS analysis was conducted. Figure 12 shows a HAADF STEM image of a cluster of silver particles, numerically marked to show positions where EELS spectra were acquired. The background subtracted EELS spectra (Fig. 13) indicated that the Ag_M edge (390 eV) is present, however, the O edge (530 eV) was not detected. (Of course, all this could be due to the dissociation of any oxide by the effect of the vacuum on this particular sample.)



12 HAADF STEM image of cluster of silver particles, showing probe locations for EELS spectra in Fig. 13: sampling interval is 18.6 nm

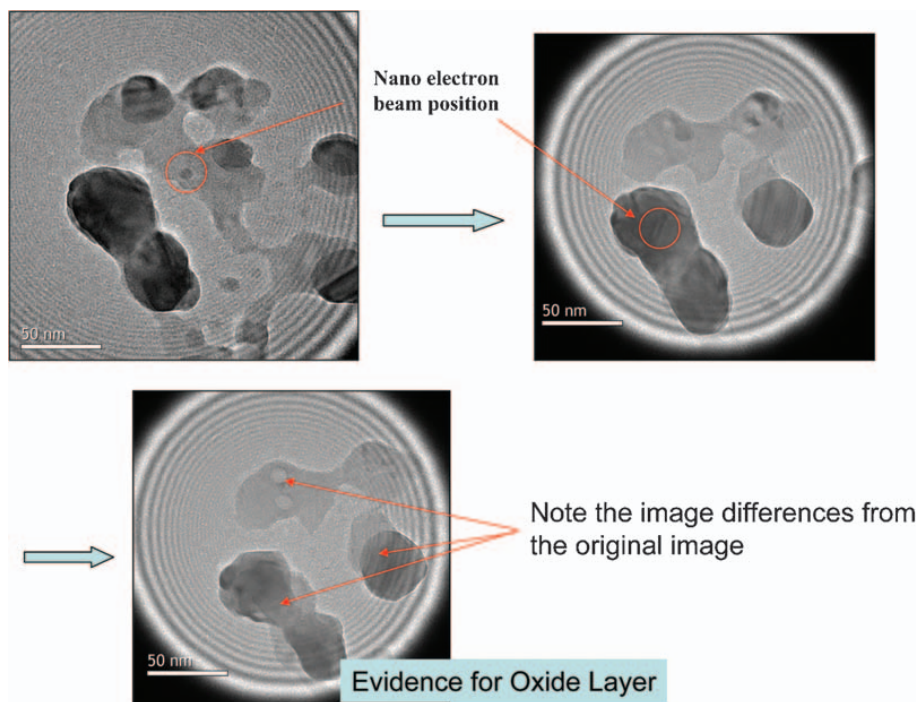


11 Electron diffraction pattern for specific grain in Silverado colloidal silver sample: pattern can be indexed as [221] of AgO phase, which has monoclinic structure; space group C2/c (Ref. 15)



13 Background subtracted EELS spectra collected from points 1, 2, 3, and 4 in Fig. 12

Support for the presence of oxygen in the solid particles as it exists in the water would be found in certain evidence for the destruction of a pre-existing



14 Background beam radiation damage on ASAP plus 22 ppm silver phase

solid oxide introduced into the beam. The SAED data appear to show this in some samples (Figs. 10 and 11). And in one or two rare samples some evidence for oxygen is found in EELS.

Moreover, one of the most telling sets of data is found by observing the effect of an electron beam on the ‘silver’ particles from the sols. Figure 14 shows a remarkable example of the beam leaving a circular imprint wherever it has been focused, as though a layer of some material, ‘oxide?’ had been evaporated (partially or wholly). Silver tarnish removal by mere heating to ~400°C has been used for generations in Europe; and this would mimic that exposure.

Perhaps the most remarkable and interesting overall observation was made in the environmental TEM, in which the samples were loaded to an environmental chamber, and water vapor was introduced into the chamber during the TEM analysis. In the starting point and the time lapsed sequence (Figs. 15), we can observe a ‘cluster particle’ of about 20 nm in size. Note the fluctuation of density. When H₂O vapor is admitted into the vacuum path (Fig. 16), the cluster dissociates into ~5 nm size particles which appear to ‘fly away’ from the core. Even more intriguing is the observation that when the column dries out again these 6–8 nm particles return and tend to re-aggregate into the larger clusters. A second intriguing observation in the cryo-TEM work at University of Washington (Fig. 17) shows that the ‘particles’ within the clusters do not touch, but arrange with a 2–3 nm (‘charge’) barrier between them. Many hypotheses are possible to explain this extraordinary observation. However, it appears that most generally there is a substructure to the larger particles of silver, and the observation that these 5–8 nm particles separate out depending on the presence of water may be very significant. The most important possible inference applies to the myriad applications of wet silver cloth, wire, etc., in medical applications.^{3,4} This would explain the role of always wetting silver cloth when used in

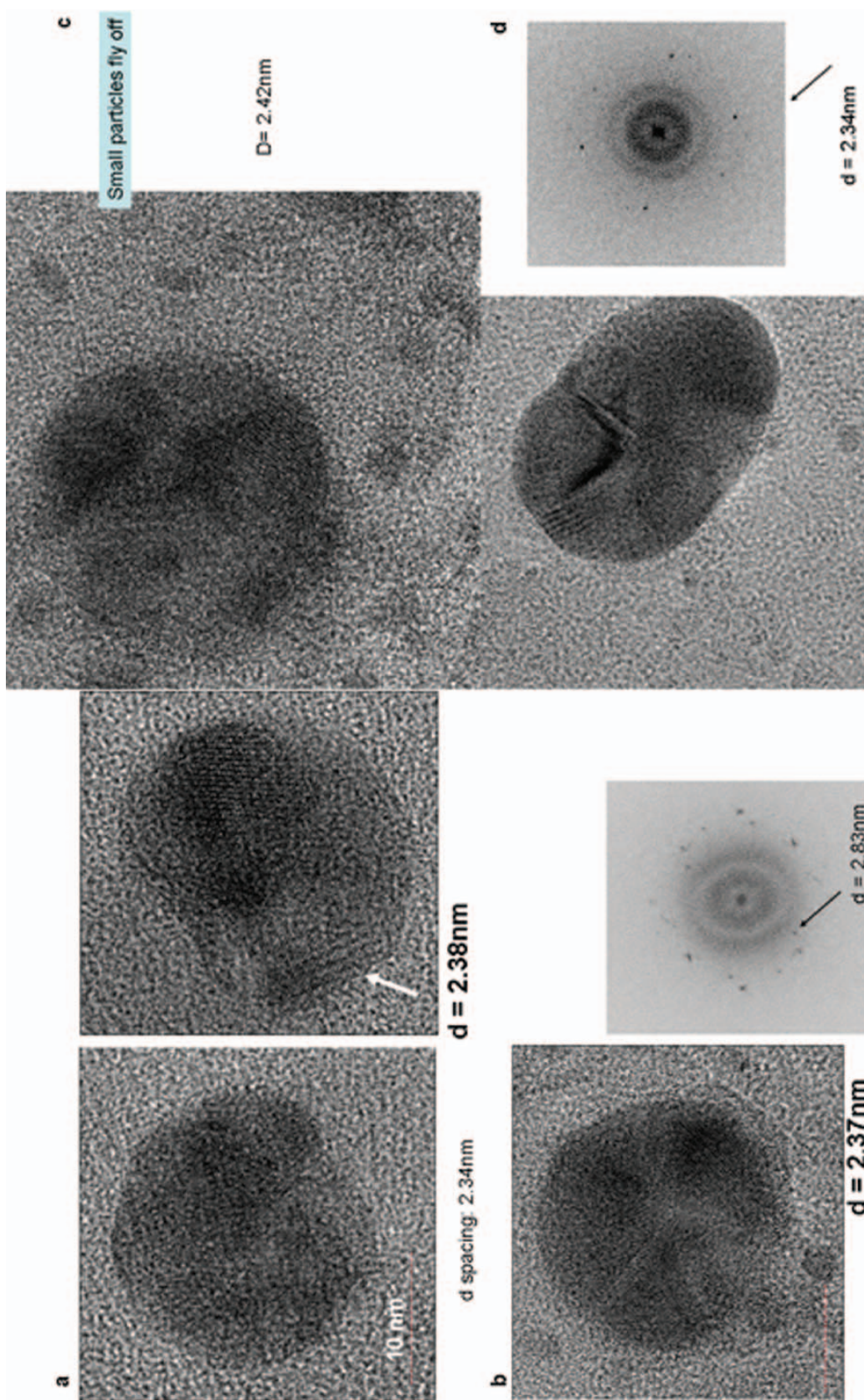
wound healing, for example. Or when silver metal is used as silver wires with the silver sol in the unique success in re-growing human limbs.⁵ The authors’ term ‘iontophoresis’ may then well refer to not ‘ions’ but to 5 nm clusters of metallic atoms which are mobilized in the field. These nano-clusters may be the typical stable unit of metal+oxide silver which is the key to its biological activity. It produces not ionic silver, but mobile 5 nm clusters of silver+silver oxide.¹⁵

Structure of liquid phase

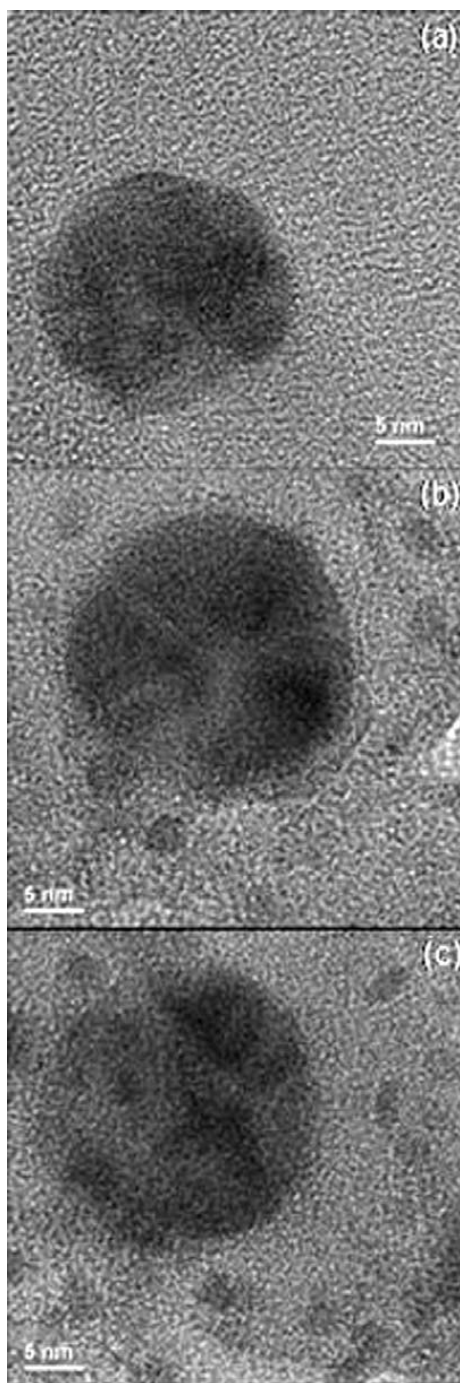
Readers interested in the liquid water phase are urged to start by studying the work on the structure of the water ‘molecules’ (not the condensed phase) which is the magisterial, regularly updated review by Chaplin.¹⁶ For those interested in the structure of *liquid* water, the recent major article by Roy is similarly needed.⁷ This work has shown that, contrary to our zeroth-order assumptions, condensed liquid water in the range of –10 to +100°C can have many different structures caused by arrangements and rearrangements of different size clusters in the 1–1000 nm range. No work has been done on the temporal stability of such liquid structures, and its relationship to nearest-neighbor molecular motions and bond vibrations is not very relevant.

The goal of this work was to see if one could demonstrate any reproducible differences between and among the starting pure water and the various sols produced from it. We believe the assigning of spectroscopic peaks to particular structural element at this stage is premature. Careful empirical data are certain to advance the basic science when and as they can be utilized.

The key tools used for studies of liquid phase structure were chiefly Raman spectroscopy, and then later, UV–VIS, and FTIR spectroscopies. In the course of this work some six different state-of-the-art Raman instruments at various locations were used: at Penn State University, Arizona State University, University of

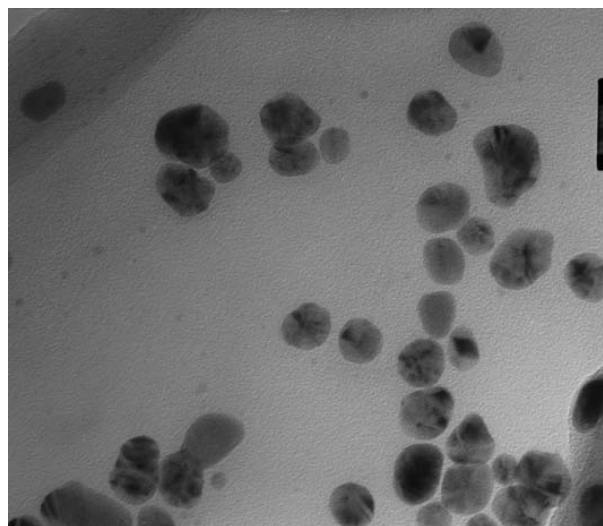


15 Time lapsed environmental TEM sequence (690k \times magnification) of silver particles following introduction of water vapor into chamber: a HRTEM images at 690k \times , particle size ~22 nm; b 1.5 torr H₂O; c 3 torr H₂O, water admitted, small particles fly off; d 3 torr H₂O, room temperature



16 Environmental TEM bright field time lapsed images of 'cluster' Ag particle in the time lapsed sequence: a without H₂O vapour; b with 1.5 torr H₂O vapour; c with 3 torr H₂O vapor introduced into environmental chamber

Puerto Rico, WITec GmbH (company headquarters in Germany), Horiba-JY (US headquarters), and General Resonance LLC. In two cases, (WITec, Horiba-JY) the analyses were performed according to the manufacturers' recommended techniques in their own laboratories. A surprising result of our work, mainly over the period 2003–2005, was that different instruments – to our chagrin – gave very different results. These results have led us to the conclusion that a single Raman spectrum on a liquid – neither ours nor any as published in a typical paper – is not in any way a reproducible general signature for that phase, as is, say, an XRD or



17 Cryo-TEM image of cluster Ag particles: note internal 'particles' do not touch

EDS pattern. These remarkable results are being reported in a longer paper elsewhere.¹⁷ They have since been fully supported in a similar conclusion from NIST.¹⁸

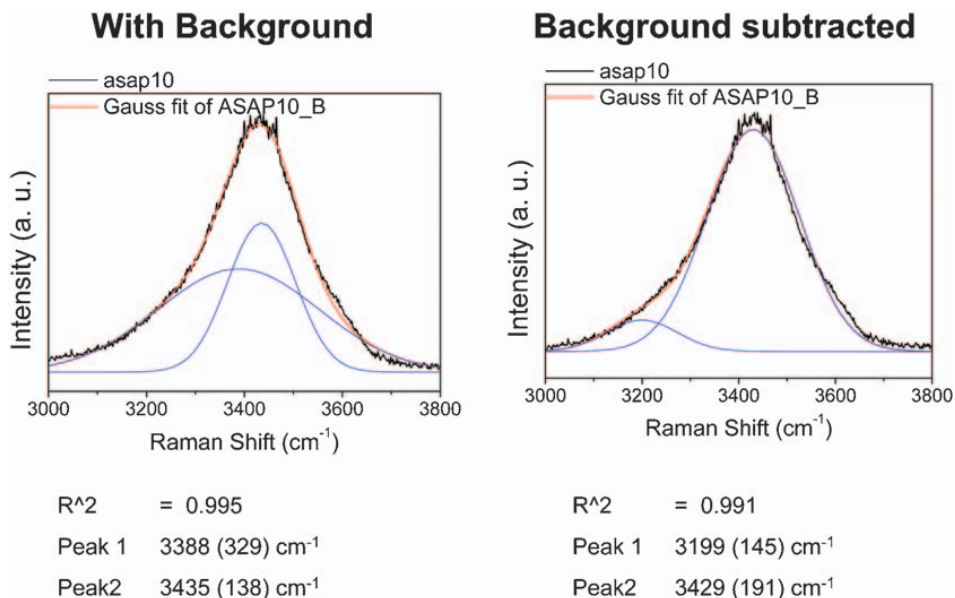
However, for the purposes of this work we were able to finally establish by tedious calibration procedures that by working on the same instrument and keeping all instrumental operational parameters fixed (including ambient room illumination) one could reproduce the results on the same machine with the same samples with different operators and with repetition at different times over a period of months. Hence, we believe that one can compare different samples with each other under identical operational conditions, and be able to rely on the reality of any differences between and among samples on the same instrument with modest confidence.

Because, as will be seen, the differences among the data from different instruments, and the differences in the spectra are so large, attempting to connect specific features to particular bonds and their charges is regarded as unjustified at the present state of our responsibility of data and our understanding of the structure of water.

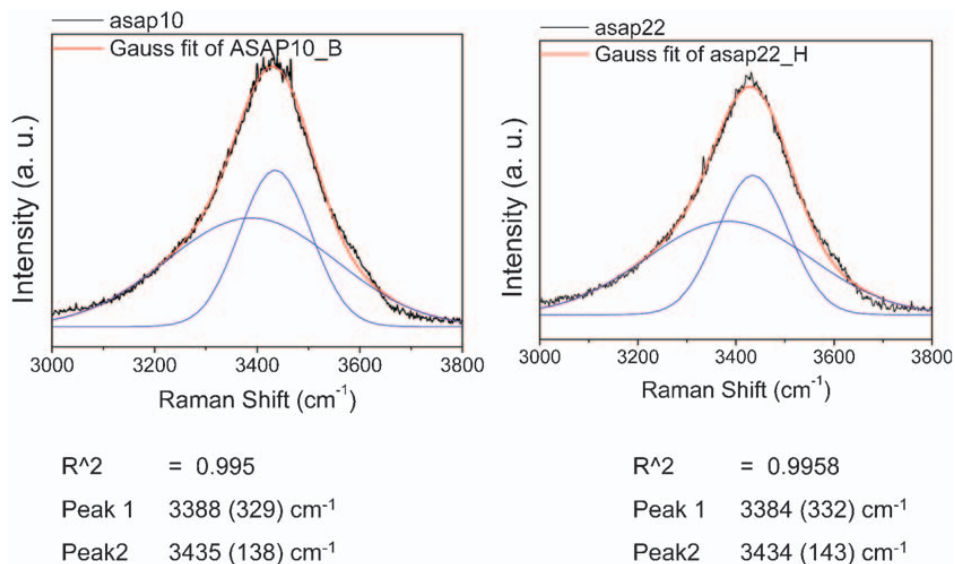
Figures 18–23 show how refinement of the data-processing achieved by deconvolution of overlapping peaks can easily be changed by assumptions and how treating the data to greater or lesser extent, e.g. background elimination or not, can cause major changes in interpretation. We made no attempts at such refinements and assignments because of the variability one gets on one's assumptions in treating the primary data.

The well-known bond-stretching absorptions are shown in Figs. 24–26 in a series of immediately repeated runs on an immersion probe instrument showing the precision attainable with no other variables. For such calibration purposes, we have run some hundreds of spectra on various 'pure' waters. While results from different instruments are never the same, even on the same sample, results obtained on repeated runs of a sample on a single instrument are nearly identical.

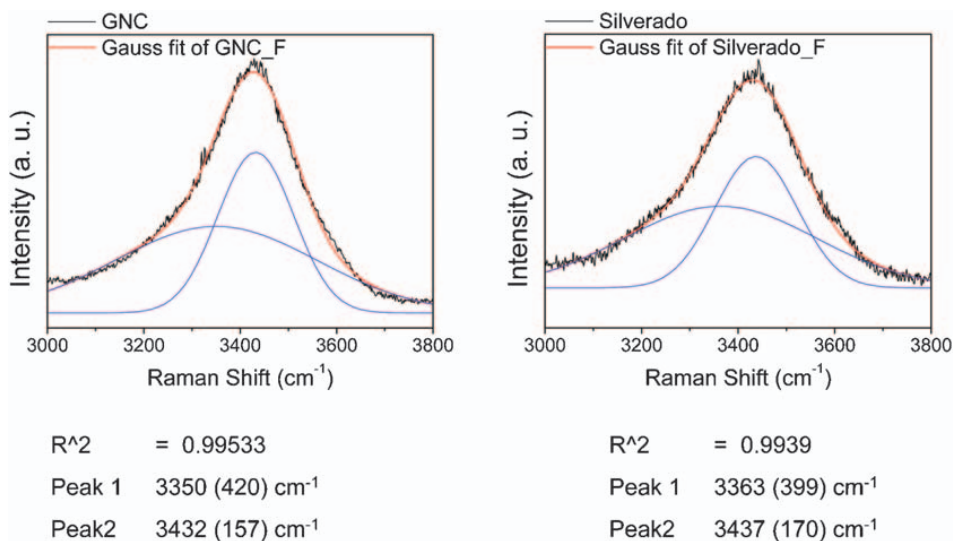
Striking differences were found on inspection of some sol samples. For example, a ASAP22 sample water droplet 10 mm in diameter on a silicon wafer run in the University of Puerto Rico, left in the laboratory ambient



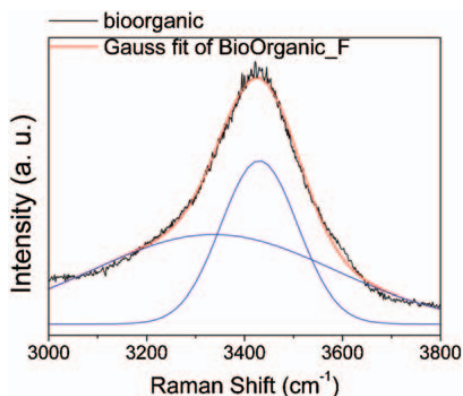
18 ASAP 10 with and without background



19 Raman spectra for ASAP 10 and ASAP 22



20 Raman spectra for GNC and Silverado



R² = 0.99512
 Peak 1 3336 (490) cm⁻¹
 Peak2 3430 (156) cm⁻¹

21 Raman spectrum for Bioorganic

for 30 days and examined periodically (and no doubt contaminated somewhat by CO₂ absorption), showed a remarkable separation of the main peaks in the main stretching mode near 3400 cm⁻¹ (Fig. 27).

This structural change was observed in an instrument which uses a containerless geometry so that surface structures are emphasized. It was also correlated with the repeated observation by different observers of the remarkable slowness of the evaporation of such drops. Of course, contamination with CO₂ or dust may have been involved. No conclusions have been drawn at this

stage but speculation of the concentration of larger molecular species at the surface has been suggested to explain both observations.

A major finding is that, generally, from the data one can say that even when the stretch modes do not show much difference, the bending modes near 1600 cm⁻¹ are much more sensitive to differences in structure. Figure 28 proves the point that one can distinguish commercial Ag colloids easily from each other, and it also reinforces the high structural reproducibility of the specific ASAP10 and 22 silver sols. Figure 26 shows the same ASAP10, 22, 32 and 201 and the original water samples run in an immersion mode InPhotonics Raman spectrometer at Penn State. The position, relative intensity and shapes of the peaks in both stretching and bending modes are again remarkably similar. Yet, surprisingly, data on the ASAP samples run on a single instrument by the same operator, over a six-month interval, showed substantial differences – especially in the bend region (1600 cm⁻¹) (Fig. 29).

UV-VIS spectra

We have shown elsewhere that often in ultradilute sols, both in water and in alcohol, UV–VIS spectroscopy often shows characteristic differences in the vibrational mode region near 300 nm better than Raman spectroscopy.¹⁹ The UV–VIS Ag aquasol data (Fig. 0) show very consistent and distinct differences between the original pure water and the 10, 22, 32, and 200 ppm Ag sols made by the electrolysis process. The consistent and roughly proportional absorptions in the 200–300 nm region reflect some structural change associated with the Ag in the liquid dispersion.

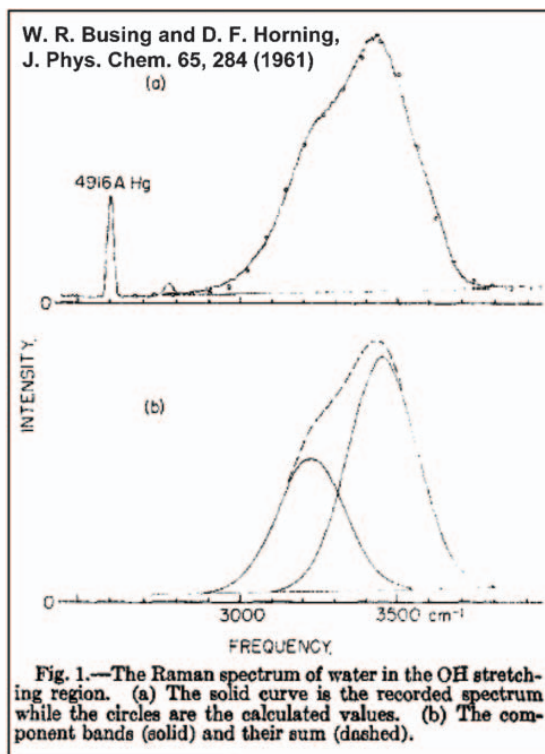
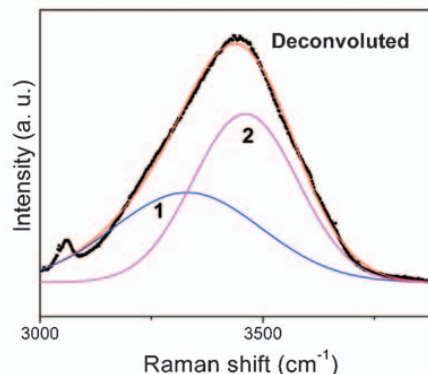
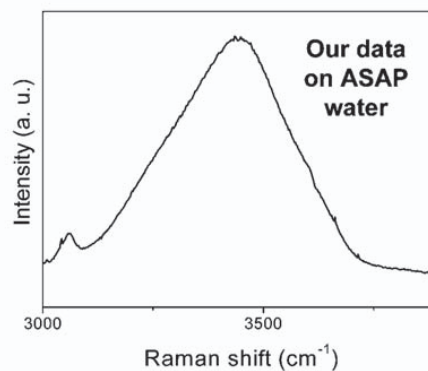


Fig. 1.—The Raman spectrum of water in the OH stretching region. (a) The solid curve is the recorded spectrum while the circles are the calculated values. (b) The component bands (solid) and their sum (dashed).

center position (FWHM)
 Peak 1 : 3225 cm⁻¹
 Peak 2 : 3450 cm⁻¹

• Correlation with ref. not good



center position (FWHM)
 Peak 1 : 3329 (331) cm⁻¹
 Peak 2 : 3460 (234) cm⁻¹

22 Comparison of Raman spectra of water²⁰ with present results for ASAP water

*D. M. Carey and G. M. Korenowski,
J. Chem. Phys. 108, 2669 (1998)

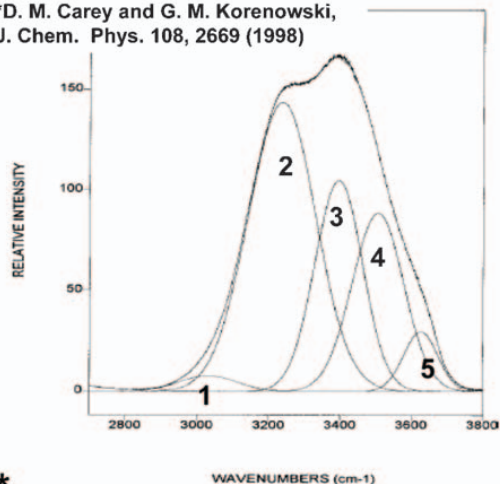
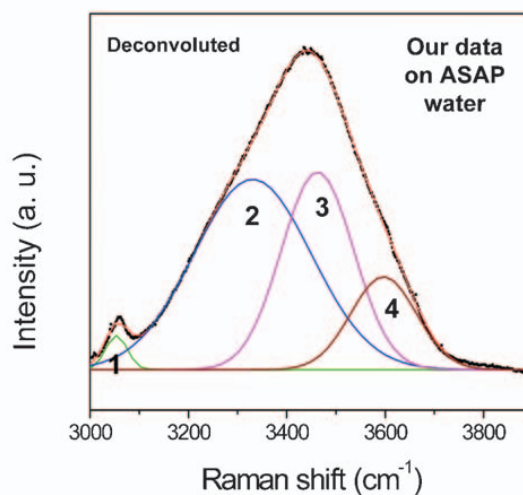


*
FIG. 5. Gaussian deconvoluted vibrational Raman spectrum of liquid water at 24 °C and 128 bar pressure in the 2700–3800 cm⁻¹ region. The reduced Chi² value for this fit was 2.51. Additional spectra at the temperatures of 200 and 400 °C are contained in the Appendix.

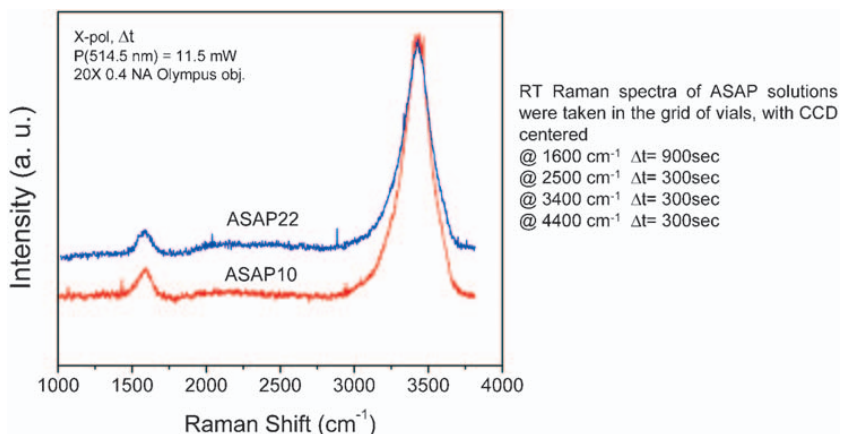
center position
Peak 1 : 3051 cm⁻¹
Peak 2 : 3233 cm⁻¹ } **Hydrogen Bonded**
Peak 3 : 3393 cm⁻¹
Peak 4 : 3511 cm⁻¹ } **Non hydrogen bonded**
Peak 5 : 3628 cm⁻¹



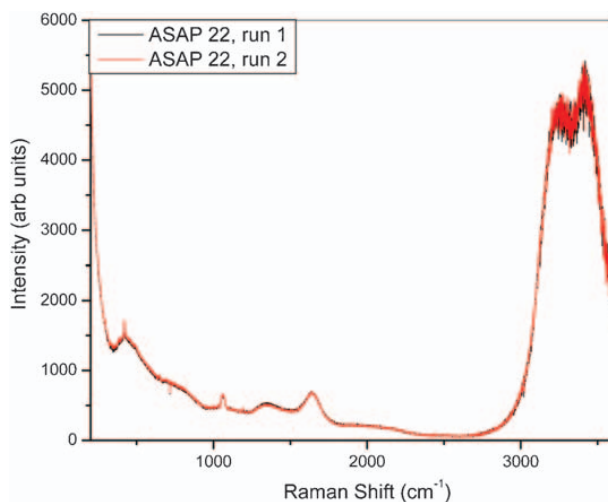
center position (FWHM)
Peak 1 : 3053 (43) cm⁻¹
Peak 2 : 3330 (239) cm⁻¹
Peak 3 : 3462 (146) cm⁻¹
Peak 4 : 3596 (133) cm⁻¹

• **Correlation with ref. good**

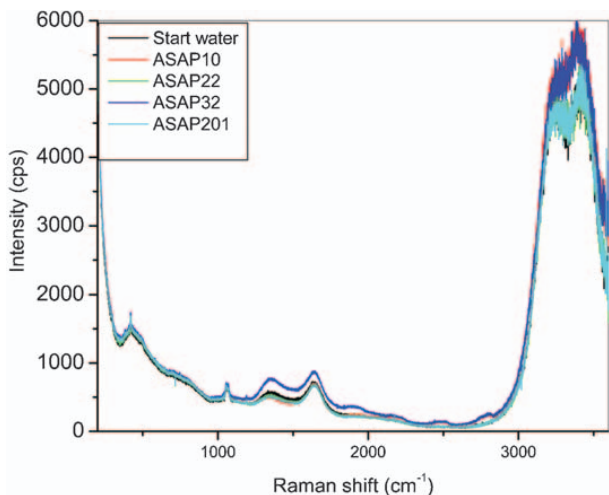
23 Comparison of Raman spectra of water²¹ with current results for ASAP water



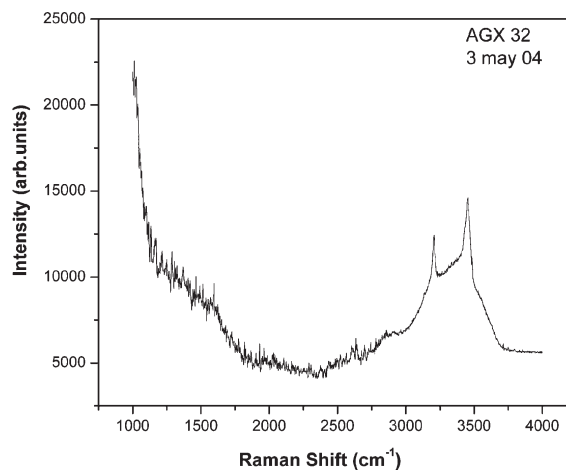
24 Raman spectra of ASAP 10 and ASAP 22: peak at ~1600 cm⁻¹ and broad peak at 3400 cm⁻¹ correspond to OH bending and stretching modes respectively; peak at 1600 cm⁻¹ is relatively weak so integration time was increased to 900 s; ASAP22 spectrum has relatively low background compared with ASAP10



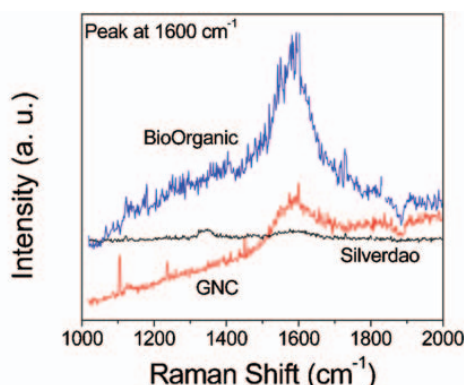
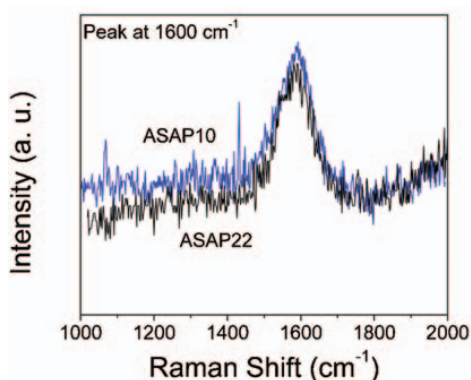
25 Two Raman spectrum runs for ASAP 22 indicating instrumental precision in data collecting



26 Raman spectra of ASAP samples with 10, 22, 32 and 201 ppm colloidal Ag

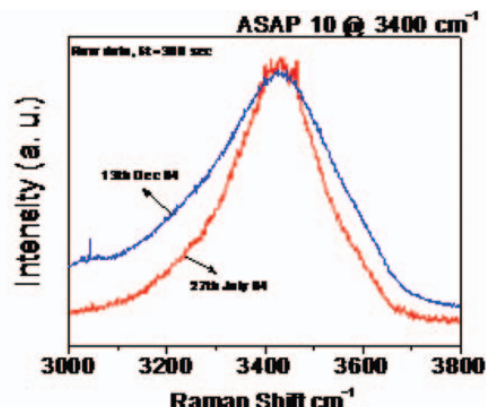
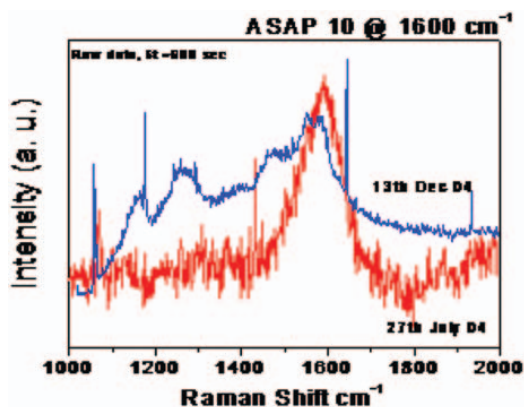


27 Raman spectra of ASAP22 sample, showing striking differences in 3400 cm⁻¹ band in containerless sample (University of Puerto Rico) instrument



X-pol, Δt = 600 sec, P(514.5 nm) = 11.5 mW, 20X 0.4 NA Olympus obj.

28 Raman spectra (1000–2000 cm⁻¹) bending modes of ASAP10, ASAP22, GNC, Silverado, and Bio Organic: clearly there is significant background in the spectra of GNC and BioOrganic, probably due to impurity scattering, and these peaks are asymmetric compared with those for ASAP solutions



29 Raman spectra of ASAP 10 ppm sample with a six-month interval

Discussion and conclusions

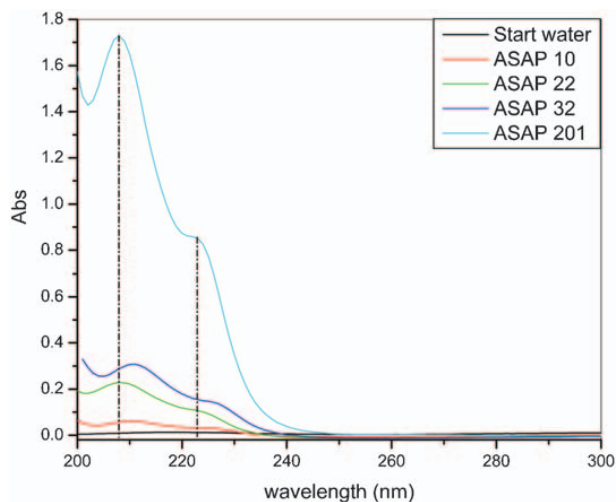
The data presented below are far from conclusive on several scientific questions which need to be answered. However, several very significant conclusions are consistent with our data.

1. The very potent biologically active silver aquasols contained, typically, the amounts of silver claimed by the manufacturer, typically from 10 to

30 ppm by weight of Ag. The silver was very pure as was the water.

2. The dominant, by far, crystalline solid phase detected in the vast majority of SEM TEM studies is metallic silver.

3. There is positive evidence for the presence of some oxygen associated with the silver—mainly as an oxide or ‘oxyhydroxide’ in the sol, yielding very small amounts of a crystalline oxide under TEM conditions.



30 Ultraviolet-visible spectra of ASAP samples showing increase in absorbance as function of Ag concentration

4. Many of the ~20–30 nm particles have a substructure with 5–7 nm particles held together by relatively weak bonds. The existence of these latter ‘mobile’, 5 nm, metallic, silver-containing units with some kind of oxide ‘layers’ or ‘skins’ around them may be a very significant finding in looking for the cause of the bio-activity.

5. Water plays a key role in ‘mobilizing’ such smaller Ag clusters, and it may be the mechanism for Becker and Flick’s so-called ‘iontophoresis’ of silver.^{3,4}

6. The spectroscopic data show that Raman spectra can often distinguish between different sol products if the spectra are run after calibration on the same instrument.

7. The differences in UV–VIS spectra between different concentrations in the range of 1 to 20 atom ppm of Ag in sols made by the same process appear to be consistent, and quite distinct.

8. Infra-red appears to be a less useful tool than Raman or UV–VIS, while UV–VIS data are consistent and clear in showing differences.

9. The data obtained point to the need for the detailed phase diagram for the phases in the system Ag–O–H₂O in the temperature range –10 to +100°C (possibly with an electric field superimposed).

Acknowledgements

We wish to acknowledge the contribution by Professor M. Sarikaya of the University of

Washington for the cryo-TEM data referred to above. Support was received from a grant from Friends of Health and the Penn State MRI initiative, and the American Biotech Laboratories, which also provided access to all their samples and data.

References

1. M. Das, S. Dixit and S. K. Khanna: *Food Additives and Contaminants*, 2005, **22**, 1219.
2. D. Storey: Proc. American Physical Society March Meeting on ‘Low temperature IPD AgO bacterial static/bactericidal coatings for various medical applications’, Baltimore, MD, 2006.
3. A. B. Flick: Proc. MRS–E/MRS-I meeting on ‘Silver healing’, Boston, MA, November 2004.
4. A. B. Flick and V. Platte: ‘Clinical applications of electrical silver iontophoresis’, Proc. 1st Int. Conf. on ‘Gold and silver in medicine’, Bethesda, MD, May 1987.
5. R. O. Becker and J. A. Spadaro: *J. Bone Joint Surg. Am.*, 1978, **60**, 871.
6. R. Roy, W. A. Tiller, I. Bell and M. R. Hoover: *Mater. Res. Innov.*, 2005, **9**, 577.
7. R. Roy: *J. Amer. Ceram. Soc.*, 1956, **49**, 145.
8. R. Roy: *Science*, 1987, **238**, 1664.
9. R. J. Holladay, H. Christensen and W. D. Moeller: ‘Apparatus and method for producing antimicrobial silver solution’, US Patent 6,214,299, 2001.
10. D. A. Revelli, D. Wall and R. W. Leavitt: ‘Antimicrobial activity of American silver’s ASAP solution’, Report, American Biotech Labs, Alpine, UT, 2000.
11. A. de Souza, D. Mehta and R. W. Leavitt: *Current Sci.*, 2006, **91**, 926.
12. Y. Xia and N. J. Halas (eds.): Special issue on ‘Synthesis and plasmonic properties of nanostructures’, *MRS Bul.*, 2005, **30**, 5.
13. O. Müller and R. Roy: *J. Less-Common Met.*, 1968, **16**, 129.
14. O. Müller, R. E. Newnham and R. Roy: *J. Inorg. Nucl. Chem.*, 1969, **31**, 2966.
15. J. R. Morones, J. L. Elechiguerra, A. Camacho, K. Holt, J. B. Kouri, J. T. Ramirez and M. J. Yacaman: *Nanotechnology*, 2005, **16**, 2346.
16. M. Chaplin: ‘The structure of water’, Proc. 2nd Int. Conf., on ‘Science of Whole Person Healing’, (ed. R. Roy), 2006, iuniverse.com.
17. M. R. Hoover, R. Roy, A. S. Bhalla, B. Srinivasan and S. Dey: ‘Highly unreliable laser Raman spectra of water from different state of the art instruments’ (in preparation).
18. S. Choquette: *American Lab*, 2005, **37**, 22.
19. R. Roy, M. L. Rao, M. R. Hoover and I. Bell: UV–VIS spectra of ultradiluted aquasols and alcosols, containing different additions’, Proc. Schwartz Report Conf., Virginia Beach, VA, November 2006.
20. W. R. Busing and D. F. Horning: *J. Phys. Chem.*, 1961, **65**, 284.
21. D. M. Carey and G. M. Korenowski: *J. Chem. Phys.*, 1998, **108**, 2669.